Proceedings of the 7th World Congress on New Technologies (NewTech'21)
~~Prague, Czech Republic~~ Virtual Conference – August, 2021
Paper No. ICEPR 114
DOI: 10.11159/icepr21.114

Chestnut Soils: A Comparison Study by Diffuse Reflectance and Attenuated Total Reflection FTIR spectroscopies with Fractionation

Dmitry S. Volkov[1], Olga B. Rogova[1,2], Mikhail A. Proskurnin[1]
[1]Chemistry Department of M.V. Lomonosov Moscow State University
Leninskie Gory, 1-3, GSP-1, 119991, Moscow, Russia
dmsvolkov@gmail.com; proskurnin@gmail.com, michael@analyt.chem.msu.ru
[2]Department of Chemistry and Physical Chemistry of Soils, V.V. Dokuchaev Soil Science Institute
Pyzhevsky per., 7/2, 119017, Moscow, Russia
obrogova@gmail.com

Abstract **-** For wet-sieving fractionated aggregates of chestnut soils (20–1000 μm) with different agricultural use (a fallow and arable land) and depth profiling, attenuated total reflection (ATR) and diffuse-reflectance (DRIFT) modalities of IR spectroscopy were used for distinguishing differences in the mineral and soil organic matter (SOM) composition. Among fractions, the differences are minimal, and the fraction of 20–400 μm bearing the maximum information volume. Both modalities are complementary: ATR provides more information on the carbonate/silicate matrix and the changes in the range of 1600–200 cm^{-1}, while DRIFT provides higher sensitivity in the hydrogen-bond and organic carbon ranges (3800–2700 cm^{-1}) and more differences in the carbonate range (1600–1400 cm^{-1}). Most changes between the agricultural-use samples are observed in upper horizons Ap, in the SOM range (3000–2800 cm^{-1}), although slight (arable land shows significantly lower amounts of total organic carbon) and in the carbonate range (1600–1300 cm^{-1}). The increase in carbonate contents with the horizon depth was found for both samples, with no significant changes in the silicate part were found.

Keywords**:** FTIR, infrared spectroscopy, chestnut soils, soil degradation, wet fractionation, soil aggregates

1. Introduction

Chestnut soils fill significant areas in Turkey, Russia, Mongolia, North China, the USA, and Argentina. The climatic conditions of the chestnut soils zone are characterized by sharp continental and arid conditions. Chestnut soils are potentially fertile, and the successful cultivation of a wide range of crops is possible: cereals (wheat, corn, barley), industrial, vegetable, fruit, provided that a set of measures for moisture accumulation is carried out. For sustainability and agricultural use, it is also necessary to protect chestnut soils from water and wind erosion, secondary salinization, and the introduction of mineral and organic fertilizers. The slowing down of the plant residue transformation process in chestnut soils compared with chernozems is reflected in the molecular weight distribution of the system of humic acids and mineral matrix components. Thus, the use of chestnut soils requires the characterization of various parameters. Over the last two decades, the role of IR spectroscopy in soils and similar studies of biochars, humic substances have dramatically increased due to advances in instrumental capabilities, new modalities, and increased sensitivity [1-3]. Comparing various modalities for soils is a topic of several review or feature papers [4, 5]. A complete comparison of attenuated total reflection (ATR) and diffuse-reflectance (DRIFT) features for chestnut soils was not made as far as we are concerned. Also advantageous is the FTIR spectroscopy approach based on preparative fractionation [6, 7]; however, such a combination is not widespread. Thus, within this study frame, we compare modality information for chestnut soil samples of different agricultural use (a fallow and arable land), five soil horizons, and wet-sieving fractionated aggregates (20–1000 μm).

2. Materials and Methods

Samples of chestnut soils (WRB, 2006; Haplic Kastanozems) were taken at the Kachalino test site, Volgograd (lower Volga) region [8] were from two sections on the fallow (over 30 years; 49.06.42 N 44.09.43 E) and arable soil under the grain crop rotation (49.05.09 N 44.06.52 E). The wormwood-fescue association represents the vegetation cover of the deposit area. The parent rocks are loess-like carbonate saline loams; the average rainfall is 380 mm/year. The total organic carbon (TOC) is 1.7–2.0 %, the carbonate content in the upper layer of 0–20 cm is 12–15%, the content of the fraction of below 1

μm, 27–30%. Mealy new formations of carbonates were opened from 40 cm, new formations of gypsum, from 80 cm. The soil samples were air-dried with no extra grinding. A weighed portion of an average sample of 50 g was dispersed in a water-filled sieve column with mesh sizes of 1000, 500, 250, 200, 100, 80, 63, 40, and 20 μm to fractionate waterproof aggregates. The aggregates remaining on the sieves were collected in evaporation bowls and dried at 35 ºC.

IR spectra were recorded on a Bruker Vertex 70 single-beam IR Fourier spectrometer (Bruker Optik GmbH, Germany) equipped with a KBr beam splitter and a wide-range room-temperature DTGS detector or liquid nitrogen cooled photovoltaic MCT detector. The spectrometer and accessories were continuously purged with –70°C dew point air (produced by a PG28L Purge Gas Generator, PEAK Scientific) with a flow of 500 L/h. The overall laboratory temperature was maintained at 23 °C with a variation of ± 1 °C using an air conditioner. A GladiATR™ single-reflection ATR accessory with a diamond crystal (Pike Technologies, USA) was used. A background signal was recorded before each new sample. The soil spectra were recorded using a wide-range silicon beam splitter in the range of wavenumbers of 4000–100 cm^{-1}; the baseline was not corrected. The PrayingMantis™ DRIFT accessory (Harrick Scientific Products, Inc.) was used. The software automatically converted spectra measured in diffuse reflectance using the Kubelka–Munk (KM) conversion. The smallest value allowed for transmittance or reflectance is 0.001% (a KM value, *ca.* 500). The tilted alignment mirror for the PrayingMantisTM accessory was used for background measurements.

3. Results and Discussion

3.1. Band Assignment

Most bands belong to quartz lattice (797 and 775 cm^{-1} [shoulder], O–Si–O stretch, 697, 510 cm^{-1}, Si–O–Si bend; 460, 450 (shoulder), 430 cm^{-1}, O–Si–O bend. Bands at 975 and 455 cm^{-1} can be attributed to amorphous silica (Figure 1). The range 1270–800 cm^{-1} contains a broad band at 1120–1070 cm^{-1}, and O–Si–O stretch in crystalline and amorphous SiO_2 species; bands at 1035 and 1010, quartz lattice O–Si–O stretch; 912; 840 (weak shoulder), Si–O^- [9]. The band at 1645–1640 cm^{-1}, shoulder band, bend (ν_2) of the covalent bonds of liquid absorbed water [10]. A shoulder band at 1395 cm^{-1} is the symmetric carboxylate stretch. In DRIFT, the triplet of 1980, 1860, and 1780 cm^{-1} is a quartz matrix signature [11, 12]. The band at 1780 cm^{-1} has an overlapped carbonate component at 1805 cm^{-1}, which is detectable in the ATR mode. Most carbonate bands agree with calcite and 2512, 1805 (combined band), 1460–1435, and 1410 cm^{-1} (asymmetric and symmetric carbonate stretch vibrations) 1090, 875, and 715 cm^{-1}. The range 3100–2800 cm^{-1} is reliably detected only by the DRIFT modality. It is comprised of alkene/aromatic sp^2 $=CH_2$ stretch; 2975 and 2885 cm^{-1}, the antisymmetric and symmetric stretch of methyl groups; 2930 and 2855 cm^{-1}, the antisymmetric and symmetric stretch of methylene groups, bands of CH_x groups are on the shoulder of the OH continuum band. A broad band in the range of 2400–3700 cm^{-1} with a maximum of about 3410 cm^{-1} is a signature band of OH vibrations of water with different hydrogen bonds. The bands in the hydrogen-speciation range are 3710 (unbonded SiO–H stretch, tilted (kaolinite, clay) [13]; 3700–3680, hydrogen-bonded SiO–H…H_2O stretch (amorphous species); and 3400 and 3270, condensed-phase antisymmetric and symmetric hydrogen-bond ensembles.

3.2. Sample Comparison

From the viewpoint of fraction sizes, it is preferable to use fine fractions to obtain more reliable results and compare them. The reproducibility of the shapes, maximum positions, and integral areas of almost all bands in both modalities are higher for a fraction of 20–40 μm. This finding agrees with the previously reported improvement in band reproducibility and spectral intensities [14]. The fractions of 20–40 μm of both agricultural-use samples provide mainly the same information as other fractions and whole soils; they can represent the whole soil.

The trends common for the two samples were found. Upper horizons (Ap, 0–25 cm) do not contain carbonate peaks, while in the transition from BC (80–130 cm) to Bca (40–80 cm) horizons, the intensities of carbonate of almost all the bands increase by ca. 10–15 times and then twofold decreases towards the Ccs (130 cm) horizon. Horizon Ap contains the minimum amounts of SOM (TOC, by the range 3000–2800 cm–1) within each sample profile, and all samples have very few organic carbonyl groups and aromatics, which distinguish them from chernozem and sod-podzolic soils [5]. The amorphous and crystalline silicon peaks change little along with the profiles; crystalline silicon probably prevails.

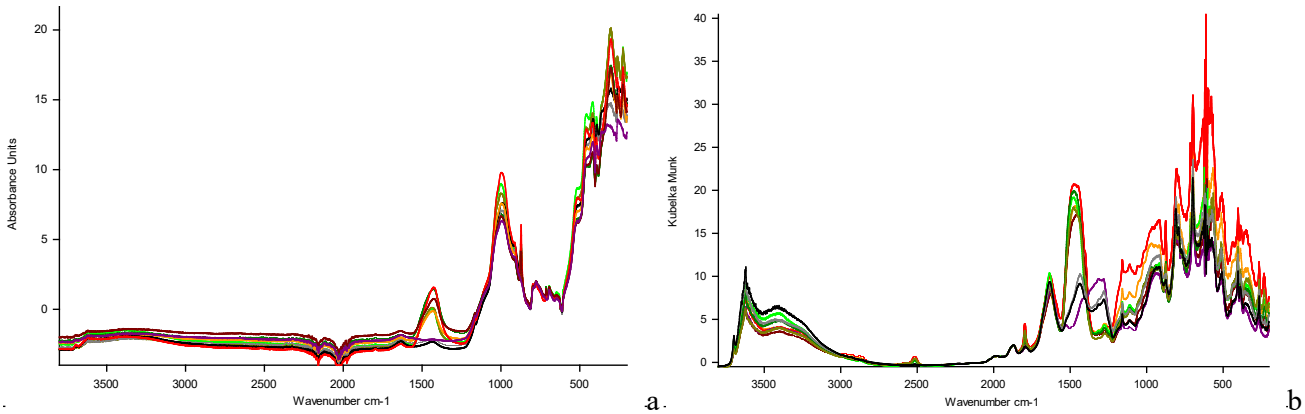

a. b

Fig. 1: ATR (a) and diffuse-reflectance (b) spectra of chestnut soils, a fraction 20–40 µm. Color code: black, arable land horizon Ap; gray, arable land horizon Ap'; khaki, arable land horizon Bca; dark green, arable land horizon BC; light green, arable land horizon CCs; magenta, fallow horizon Ap; dark red, fallow horizon B1; light red, fallow horizon Bca; orange, fallow horizon Bccs.

Possibly, with depth, the proportion of hydrocarbonates increases (manifestation of C–OH groups). Differences in the lowest horizons (except for the CHx content) are minimal. Water contents by bend and libration bands do not significantly change along with the depth profile. The difference between fallow and arable samples is rather distinct. The fallow contains much more significant amounts of organic matter having a larger number of methylene groups (2930 and 2855 cm–1), i. e., longer hydrocarbon chains and a more significant amount (and more significant growth along with the profile) of biogenic silicon (1270–1150 cm–1) [15]. Fallow also shows a more substantial SOM content increase with depth. As it is a fallow where the natural soil formation processes have been restored for 30 years, and new organic matter is not removed, it is humified and accumulates naturally for these soils. The growth of SOM with depth (up to certain limits, down to B1 horizon) is associated with the transfer of SOM in the composition of clayey cutans, which determines the textural differentiation of chestnut soils with signs of alkalinity [16]. In both soils, the accumulation of carbonates in the Bca horizon is morphologically shown; the lowest horizon is gypsum-bearing, although no distinct bands attributed to gypsum are found in IR spectra. Arable land in the upper horizons Ap and Ap' contains a carbonate peak at 1430 cm–1 compared to the position at 1460 cm–1 in lower horizons and the fallow sample. It can be the manifestation of the domination of calcite and ammonium carbonate. The band deconvolution shows the maximum of 1390 cm–1 characteristic to nitrate from nitrogen fertilizers [17] applied to the upper arable horizon in the arable-land sample. A change in the carbonate can be plowed from the underlying layer. While there is almost no carbonate in the horizon in the Ap horizon of fallow, then the horizons of both samples level out to calcium carbonate attributed to dolomite (1460–1450 cm–1) [18] characteristic for the underlying rock formations in the sampling area. Apart from the upper horizons, the most different from all the remaining is the Bca horizon.

3. Conclusion

The considered approach to the IR analysis of aggregates fractionated by sieving allows assessing changes in the composition of soils under various factors. Fine soil fractions µm result in the maximum sensitivity, reproducibility showing no changes from larger fractions by the information contents, and representative samples for analysis. It can be used in estimating an external impact or depletion because of extensive agricultural use (degradation) or restoration of structure and properties when using non-dump and intensive agricultural technologies.

Acknowledgements

This work was supported by the Russian Science Foundation, grant no. 19-13-00117. This research was performed according to the Development program of the Interdisciplinary Scientific and Educational School of Lomonosov Moscow State University, "The future of the planet and global environmental change".

References

[1] L. M. Fultz, J. Moore-Kucera, F. Calderón, and V. Acosta-Martínez, "Using Fourier-Transform Mid-Infrared Spectroscopy to Distinguish Soil Organic Matter Composition Dynamics in Aggregate Fractions of Two Agroecosystems," *Soil Sci. Soc. Am. J.,* vol. 78, no. 6, pp. 1940-1948, 2014, doi: 10.2136/sssaj2014.04.0161.

[2] Y. Ge, J. A. Thomasson, and C. L. S. Morgan, "Mid-infrared attenuated total reflectance spectroscopy for soil carbon and particle size determination," *Geoderma,* vol. 213, pp. 57-63, 2014, doi: 10.1016/j.geoderma.2013.07.017.

[3] A. Tinti, V. Tugnoli, S. Bonora, and O. Francioso, "Recent applications of vibrational mid-Infrared (IR) spectroscopy for studying soil components: a review," *Journal of Central European Agriculture,* vol. 16, no. 1, pp. 1-22, 2015, doi: 10.5513/jcea01/16.1.1535.

[4] S. Pasieczna-Patkowska and J. Madej, "Comparison of photoacoustic, diffuse reflectance, attenuated total reflectance and transmission infrared spectroscopy for the study of biochars," *Polish Journal of Chemical Technology,* vol. 20, no. 4, pp. 75-83, 2018, doi: 10.2478/pjct-2018-0057.

[5] P. K. Krivoshein, D. S. Volkov, O. B. Rogova, and M. A. Proskurnin, "FTIR photoacoustic spectroscopy for identification and assessment of soil components: Chernozems and their size fractions," *Photoacoustics,* vol. 18, p. 100162, 2020, doi: 10.1016/j.pacs.2020.100162.

[6] M. Pansu and J. Gautheyrou, "Characterization of Humic Compounds," in *Handbook of Soil Analysis: Mineralogical, Organic and Inorganic Methods*. Berlin, Heidelberg: Springer Berlin Heidelberg, 2006, pp. 399-451.

[7] B. T. Christensen, "Physical Fractionation of Soil and Organic Matter in Primary Particle Size and Density Separates," in *Soil Restoration*, B. A. Stewart Ed., (Advances in Soil Science. New York, NY: Springer New York, 1992, ch. Chapter 1, pp. 1-90.

[8] R. Kurbanov, A. Murray, W. Thompson, M. Svistunov, N. Taratunina, and T. Yanina, "First reliable chronology for the Early Khvalynian Caspian Sea transgression in the Lower Volga River valley," *Boreas,* vol. 50, no. 1, pp. 134-146, 2021, doi: https://doi.org/10.1111/bor.12478.

[9] S. Lucas, M. T. Tognonvi, J. L. Gelet, J. Soro, and S. Rossignol, "Interactions between silica sand and sodium silicate solution during consolidation process," *Journal of Non-Crystalline Solids,* vol. 357, no. 4, pp. 1310-1318, 2011/02/15/ 2011, doi: https://doi.org/10.1016/j.jnoncrysol.2010.12.016.

[10] J. J. Max and C. Chapados, "Isotope effects in liquid water by infrared spectroscopy. III. H2O and D2O spectra from 6000 to 0 cm(-1)," *J. Chem. Phys.,* vol. 131, no. 18, p. 184505, Nov 14 2009, doi: 10.1063/1.3258646.

[11] A. M. Hofmeister and J. E. Bowey, "Quantitative Infrared Spectra of Hydrosilicates and Related Minerals," *Mon. Not. R. Astron. Soc.,* vol. 367, no. 2, pp. 577-591, 2006, doi: 10.1111/j.1365-2966.2006.09894.x.

[12] D. S. Volkov, O. B. Rogova, and M. A. Proskurnin, "Photoacoustic and photothermal methods in spectroscopy and characterization of soils and soil organic matter," *Photoacoustics,* vol. 17, p. 100151, Mar 2020, doi: 10.1016/j.pacs.2019.100151.

[13] P. J. Heaney, A. K. Kronenberg, C. T. Prewitt, and G. V. Gibbs, "Chapter 4. Hydrogen Speciation and Chemical Weakening of Quartz," in *Silica*: De Gruyter, 1994, pp. 123-176.

[14] B. Udvardi, I. J. Kovacs, T. Fancsik, P. Konya, M. Batori, F. Stercel, G. Falus, and Z. Szalai, "Effects of Particle Size on the Attenuated Total Reflection Spectrum of Minerals," *Appl. Spectrosc.,* vol. 71, no. 6, pp. 1157-1168, Jun 2017, doi: 10.1177/0003702816670914.

[15] X. Liu, S. M. Colman, E. T. Brown, E. C. Minor, and H. Li, "Estimation of carbonate, total organic carbon, and biogenic silica content by FTIR and XRF techniques in lacustrine sediments," *J. Paleolimnol.,* vol. 50, no. 3, pp. 387-398, 2013/10/01 2013, doi: 10.1007/s10933-013-9733-7.

[16] I. A. Gorbunova and T. A. Puzanova, "System study of arid territories and genetic features and classification criteria for separation of arid soils in the territory of Russia," *Arid Ecosystems © 2006* vol. 12, no. 29 2006.

[17] N. Rogovska, D. A. Laird, C.-P. Chiou, and L. J. Bond, "Development of field mobile soil nitrate sensor technology to facilitate precision fertilizer management," *Precision Agriculture,* vol. 20, no. 1, pp. 40-55, 2019/02/01 2019, doi: 10.1007/s11119-018-9579-0.

[18] S. Gunasekaran, G. Anbalagan, and S. Pandi, "Raman and infrared spectra of carbonates of calcite structure," *Journal of Raman Spectroscopy,* vol. 37, no. 9, pp. 892-899, 2006, doi: https://doi.org/10.1002/jrs.1518.